

BIOMECHANICAL RESPONSES TO ANKLE PERTURBATIONS DURING ELECTRICAL STIMULATION OF MUSCLE

Robinson, C.J.^{1,2}, Flaherty, B.^{1,4}, Agarwal, G.C.^{3,4}, Gottlieb, G.L.⁵

¹Rehabilitation R&D Center, Hines VA Hospital, Hines, IL, USA;

²Dept. of Neurology, Loyola Univ., Maywood, IL, USA;

³Dept. of Electrical Eng. & Comp. Sci, Univ. of Illinois, Chicago, IL, USA;

⁴Dept. of Bioengineering, Univ. of Illinois, Chicago, IL, USA; and

⁵Dept. of Physiology, Rush Medical School, Chicago, IL, USA

ABSTRACT

Compliance characteristics of the ankle were investigated in an individual with complete paraplegia at the T-6 level and in a neurologically intact individual using various constant velocity perturbations against a plantarflexed torque bias that was achieved by electrical stimulation of the soleus. These responses were compared with those obtained via a volitional plantarflexed bias in the neurologically intact. The responses were modelled using a second order linear differential equation whose coefficients were calculated from a least squares fit of measured displacement, torque and acceleration. For the paraplegic subject, this model provided an adequate description; and the values for the spring coefficient (and the corresponding natural frequency) varied linearly over the range of perturbation velocities tested (13.3 to 100 deg/sec). In contrast, the viscous damping coefficient (and zeta, the damping ratio) were non-linearly dependant on velocity.

The second order linear model failed under both the stimulated and volitional conditions in the neurologically intact. Some preliminary thoughts on this observation are presented.

KEY WORDS: Electrical Muscle Stimulation, Modelling, Compliance, Joint Mechanics

INTRODUCTION

Electrical stimulation of muscle has been proposed as a technique to restore function to paralyzed muscles. But, from a control standpoint, little is known about how

such artificial activation interacts with the still intact spinal reflex loops. We have developed instrumentation to measure and compare ankle compliance and muscle EMG activity when the ankle is subjected to perturbations in torque or angular position from bias positions that are achieved volitionally or via electrical muscle stimulation.

We are interested in determining if the compliance characteristics of the joint, under both stimulated and volitional control, can be adequately described by a second order linear differential equation of the form:

$$T(t) = Ja(t) + Bv(t) + K\Theta(t) + C \quad (1)$$

Where:

$T(t)$ = measured torque

J = moment of inertia

$a(t)$ = measured angular acceleration

B = viscous damping coefficient

$v(t)$ = angular velocity (calculated)

K = stiffness coefficient

$\Theta(t)$ = measured angular displacement, and

C = constant torque bias (calculated).

The total moment of inertia is the sum of two parallel elements, the foot and the testing device,

$$J = J_f + J_d \quad (2)$$

where:

J_f = rotational inertia of the foot with respect to the axis of ankle rotation and

J_d = inertia of the testing device.

The system parameters, such as the natural frequency and the damping coefficient can be calculated by

$$f(\text{Hz}) = \frac{1}{2\pi} \sqrt{\frac{K}{J}} \quad (3)$$

and

$$\zeta = \frac{B}{2\sqrt{KJ}} \quad (4)$$

If the compliance characteristics can be so described, is there a difference in B and K values between torque biases achieved volitionally and those achieved via stimulation? And, what role do the passive properties of the joint and muscle and the neuronal reflexes play in the compliance characteristics?

To answer these questions we have developed instrumentation to examine electromyographic and mechanical responses to angle and torque perturbations applied to the ankle joint (4). We present here some analysis techniques and prelimi-

nary results to constant velocity perturbation experiments. We present results from one subject with T6 complete paraplegia, and another subject who was neurologically intact. A total of six ankles have been tested so far with this protocol.

METHODS

Hardware and Control

The overall ankle perturbation system design is illustrated in Figure 1. A four horsepower PMI Torque Motor (Model JR24M42CH) is rigidly mounted on an aluminum bracket that is attached perpendicularly to an aluminum base plate. The shaft of the Torque motor is coupled to the footplate shaft via a LeBow Rotary Torque Sensor (Model 2121, rated load = 113 Nm). The footplate itself pivots on thrust bearings inserted into two brackets attached to the baseplate. The foot is positioned in the test device such that the medial malleolus of the ankle is centered on the axis of rotation of the device. Footplate acceleration is measured by an accelerometer (Endevco Model 7265A-HS) placed at the toe area of the footplate and aligned along the axis of rotation. Footplate displacement is measured by a Transtek rotary capacitive transducer (Model 0603-0001) attached axially to the footplate shaft and secured to the end footplate mounting bracket. A similar Transtek transducer, mounted axially at the motor end of the shaft, provides a measure of motor angular displacement for use in feedback control of the motor. This feedback control allowed the production of precise constant velocity perturbations used in this experiment.

A number of safety features are built into the perturbation system. Electrical limit-switch safety stops are attached to the motor mounting bracket and are activated by adjustable cams on the shaft. An arm extends perpendicularly from the shaft between the motor and torque sensor. The excursions of this arm, and hence of the footplate, are controlled by two adjustable mechanical stops. During an experiment, the foot under test is placed in a orthopedic shoe which has a velcro fastening strip is centered longitudinally on its flat wooden sole. A matching velcro strip is centered on the footplate. This arrangement is used to provide breakaway capability should a spasm occur.

Each position transducer is aligned so that zero volts output represented a 20° elevation of the footplate toe (which would place an ankle joint at 90°, the neutral angle for a sitting subject). The signal conditioners are adjusted to provide a gain of 5°/volt. The factory calibration of the torque transducer was verified by placing known weights on the toe of the foot plate and measuring the moment arm. Its output signal is adjusted to be 5 Nm/volt. The accelerometer was calibrated by measuring the difference in output voltage when the accelerometer was inverted with respect to gravity. This calibration was verified by applying a sinusoidal input to the system and comparing peak-to-peak displacement and acceleration. The output is set at 2500°/sec²/volt.

A Zenith model 152 (IBM XT compatible) computer is used to display torque and position graphically to the subject via a linear scale, cursor. If the experiment requires the subject to voluntarily produce a precise torque, a target can be displayed which corresponds to the desired torque. A PC's Limited 286 (AT-compatible) computer controls the perturbation system, gates the electrical muscle stimulator when

indicated, handles archival data acquisition, analysis and display, and provides near-real-time display of measured variables of interest. The overall schematic and equipment calibration of the control and measurement electronics has been presented elsewhere (4).

An artifact suppression stimulator and signal conditioner (DEM, Leini, Italy) simultaneously stimulates the soleus and records electromyographic (EMG) signals from the tibialis anterior and soleus muscles. Two 4-bar active recording electrodes produce two pairs of double-differential EMG channels that are blanked to suppress the stimulus artifact when a stimulus pulse is delivered. An isolated voltage proportional to the stimulation current is available and is monitored. Stimulation is via surface electrodes located proximal to the recording electrodes. A ground strap is located between stimulating and recording electrodes. Details of the stimulator and its design are given in Knafitz and Merletti(1).

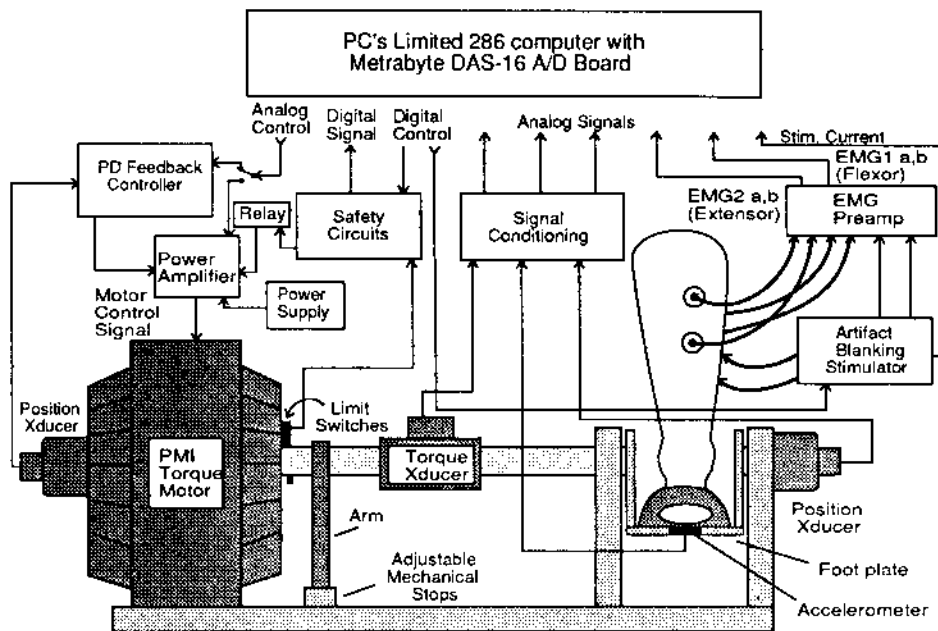


Figure 1. Ankle Perturbation System with Signal Conditioning

Experimental Design

We applied to the ankle under test a series of twelve constant velocity perturbations. Displacements were fixed at 10° and velocities ranged from 13.3 deg/sec to 100 deg/sec in six steps, each repeated twice in random order. The displacements were centered about the neutral position of the ankle (90° between the tibia and the sole of the foot). After a 1 sec hold at peak displacement, the perturbation was reversed at the same speed (see Fig. 3A,B). For this experiment, we present the results where

the foot was first dorsiflexed and then plantarflexed; the converse procedure yielded similar results.

For subjects who could produce voluntary movements, perturbations were applied against torque biases produced either volitionally or by stimulation. The instruction to the subject for the perturbations given during the voluntary torque bias was to "maintain the same effort." Stimulation current was adjusted to be tolerable and to produce up to 5 Nm of torque. Stimulation was done first, so that the torque bias could be matched volitionally for subsequent testing. For subjects with no voluntary control, torque biases were produced only by stimulation. If used, the stimulator was turned on 3 seconds before the presentation of each perturbation and turned off after 6 seconds of stimulation. Eighteen seconds elapsed before the stimulator was turned on again. Stimulation frequency was 20 Hz and the pulse width was 400 μ sec for all experiments.

Signal Processing

The mechanical values (acceleration, angle and torque) were digitized and stored at 500 Hz (12 bits) and displayed on-line to the experimenter, converted off line to their respective real values, digitally low-pass filtered (100 Hz Blackman window filter), and plotted. The EMG channels were digitized at 500 Hz (12 bits), displayed and stored, and later full wave rectified, filtered with a centered twenty point moving average filter, scaled and plotted against time. Torque, angle and acceleration were plotted against time and each other. Velocity was calculated from angle data by a single point backwards difference filter.

The coefficients J , B , K and C of equation 1 were estimated graphically by plotting torque versus angle and torque versus acceleration. In addition, since $T(t)$, $a(t)$ and $\Theta(t)$ were measured and $v(t)$ was calculated from $\Theta(t)$, the coefficients were estimated by fitting all, or a portion of, the perturbation response with a least squares approximation.

The contribution of the passive characteristics of the joint could be separated from those produced by reflex activation by examining the response of the joint in the first 100 msec of the perturbation before any spinal reflex could produce a significant mechanical response (Gottlieb and Agarwal (2)). The latency of electrical response of the triggered reflex could be verified by inspection of the EMG data.

RESULTS

Testing device calibration

The testing device, without the foot in place, is purely inertial with negligible viscous damping and stiffness. At the slowest velocity used (13.3°/sec), acceleration is minimal. And, torque is constant through the rise, hold and fall of the perturbation (Figure 2A). Thus torque has no dependence on angle or direction indicating an insignificant spring constant and viscous damping coefficient for the device. At the highest velocity used (100°/sec) the acceleration term predominates and there is a nearly linear relationship between torque and acceleration (Figure 2B). A least squares

fit ($r^2 = 0.816$) of the data in Figure 2B yields a slope of $3.66 \times 10^{-4} \pm 0.09 \times 10^{-4}$ Nms²/deg (which equals to 0.021 kgm^2). The estimated value of J via the least squares fit of equation (1) for the fastest ramp is 3.67×10^{-4} Nms²/deg.

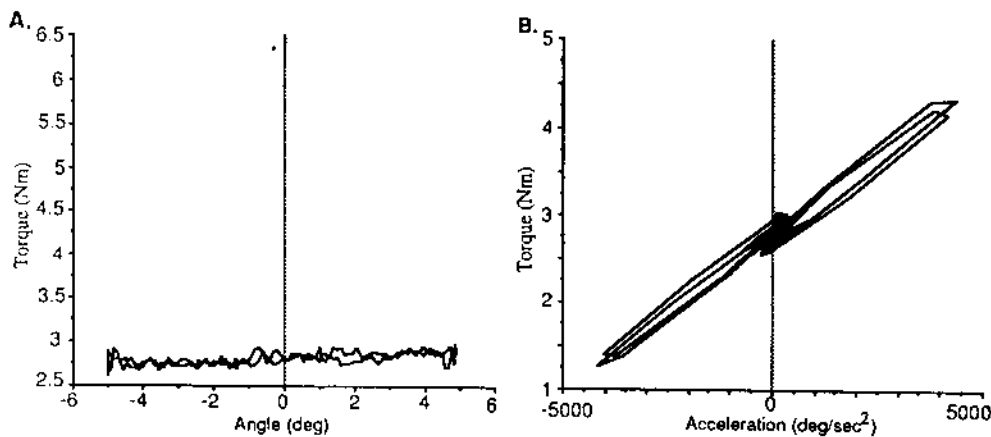


Figure 2. A) Measured torque vs measured rotational displacement for a 10° upward displacement at $13.3^\circ/\text{sec}$, followed by a 1 sec hold, and a 10° downward displacement at $13.3^\circ/\text{sec}$ to the original starting point. Note that torque has very little dependence on angle; B) Torque plotted against acceleration for the fastest velocity used, $100^\circ/\text{sec}$.

Calculation of J , B and K parameters

We investigated the compliance characteristics of an ankle of a subject with complete paraplegia (at the T6 motor level, 13 years post injury) but with intact lower motor neurons. Figure 3 shows typical results from this subject for the fastest and slowest perturbations. The area enclosed in the torque versus angle plots (Figures 3C,D) is proportional to the energy lost during the perturbation, and indicates that there is a viscous loss in the joint movement. The fact that torque and angle have the same linear relationship during the constant velocity portion of the perturbation (Thick line in Figure 3C,D, and linear region of Figures 5C,D) shows that the compliance characteristics of the joint at this amplitude of stimulation are dominated by the visco-elastic properties of the joint.

Since it is difficult to see the constant velocity portion of the perturbations we have expanded the rising portion of the perturbation (from mark 2 to mark 7) for both the slow and fast perturbations in Figure 4. Acceleration is negligible during the entire perturbation for the slowest velocity, while it is significant between marks 2 to 4 and 5 to 7 for the high velocity perturbation. Between mark 4 and 5 the acceleration value is near zero and the torque response is solely due to the visco-elastic properties of the joint. Note that for the fastest perturbation, there is a reflexive response visible in the soleus EMG occurring about 90 msec after the onset of the perturbation. The torque produced by this reflex will not have any effect until about 120 msec after the onset of the perturbation, well after the end of the perturbation. Thus the torque response to this perturbation is due entirely to the steady-state properties of the joint.

By plotting torque versus acceleration we can get an estimate of the inertia of the device and foot from the fastest velocity perturbation (Figure 5B). Between mark 2 and 4 and 5 and 7 the torque produced is mostly due to the acceleration of the inertia. The slope of the line between mark 2 and 3 (13 data points) in Figure 5B is $5.12 \times 10^{-4} \pm 0.03 \times 10^{-4} \text{ Nms}^2/\text{deg}$. The estimated value of J via the least squares fit of equation (1) over marks 2 through 7 for the fastest ramp is $4.91 \times 10^{-4} \text{ Nms}^2/\text{deg}$. Note that the acceleration for the slowest velocity perturbation is insignificant and is of the same magnitude as that of the measurement noise (Figure 5A).

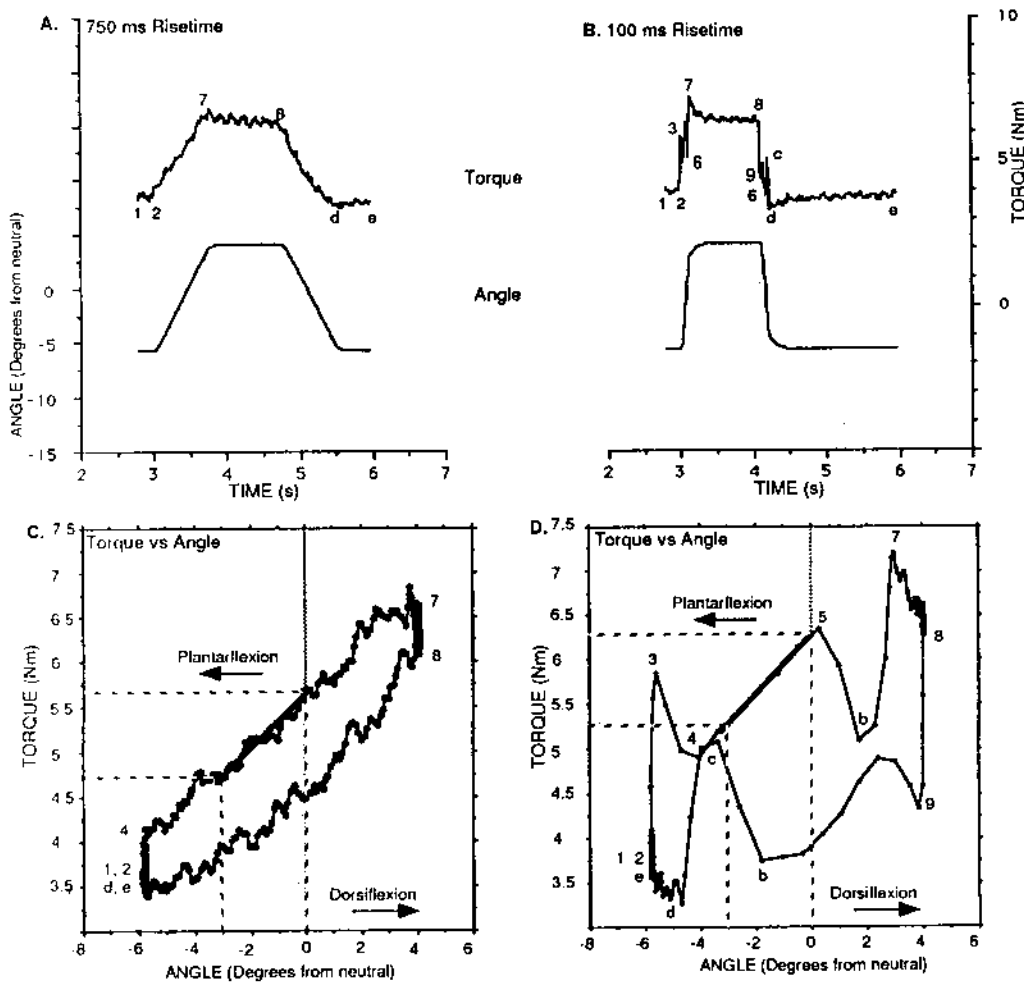


Figure 3. A,B) Plots of the angular perturbation pulses and the resultant torques for the slowest and fastest velocities used. C,D) Plots of torque vs. angular displacement over the entire perturbation cycle depicted in A and B. The small numbers and letters in each figure denote various points in the perturbation cycle.

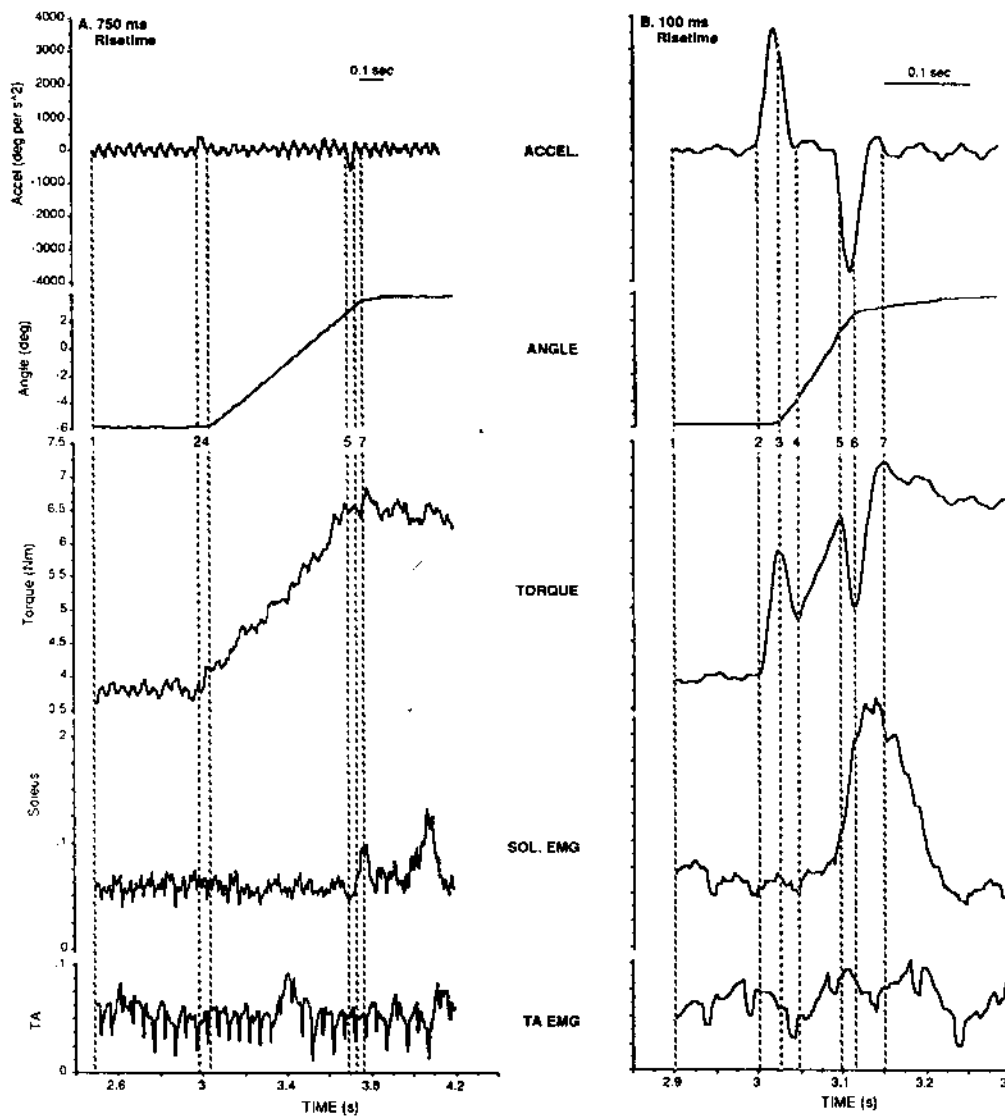


Figure 4. An expansion of Figures 3A,B, where the measured acceleration, angular displacement, torque and soleus and tibialis anterior EMGs have been expanded during dorsiflexion. Note that A and B have differing time scales. The small numbers in each figure denote various points in the perturbation cycle (c.f. Figure 3).

The stiffness for the joint can be estimated by plotting torque versus angle. The slope of the line during the constant velocity part of the perturbation is the stiffness (K) of the joint. This is estimated from the 24 data points between marks 4 and 5 Figure 5D to be 0.33 ± 0.003 Nm/deg. The stiffness of the joint was estimated using a least squares fit of equation (1) to the data from marks 2 through 7 for the fastest perturbation and found to be 0.335 Nm/deg. For the slowest ramp (Figure 5C), the slope of the line between marks 4 and 5 (320 data points) was 0.284 ± 0.002 Nm/deg. From a fit of Equation (1) to the slowest ramp data, K was calculated to be 0.279 Nm/deg.

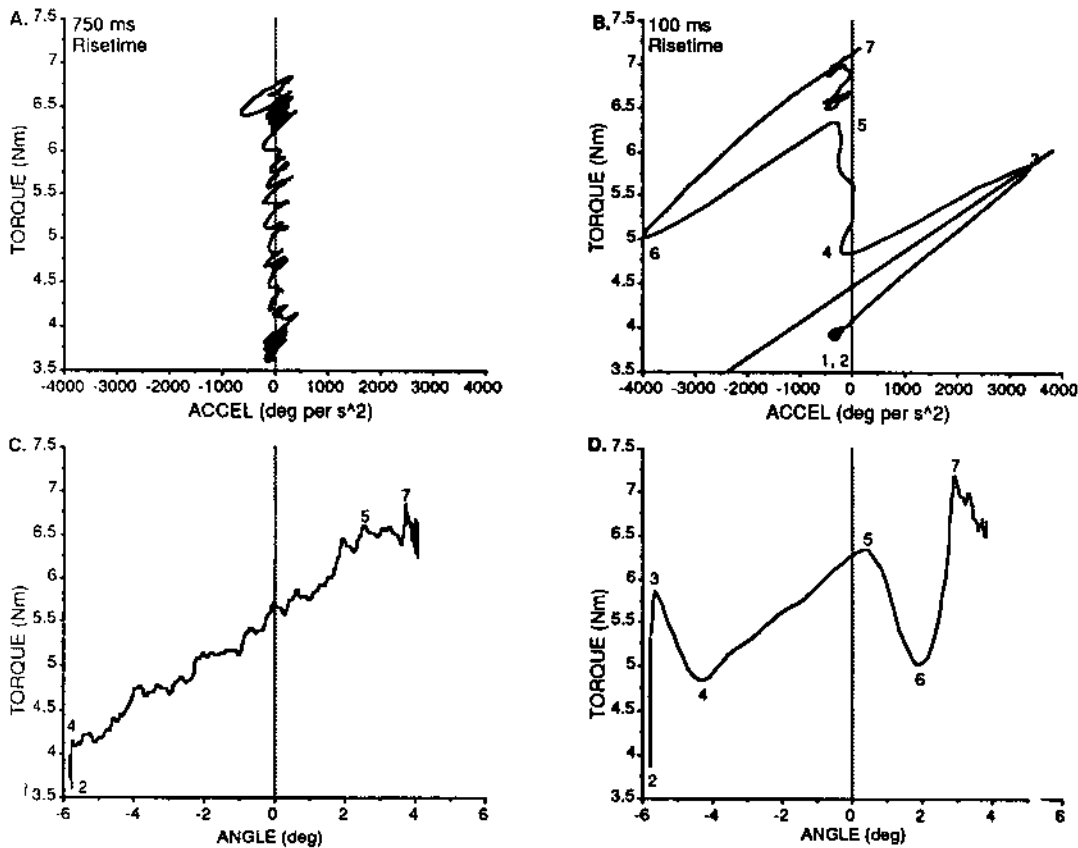


Figure 5. A,B) Torque plotted as a function of acceleration over the range between marks 1 and 7 in Figure 3. Note that torque had no dependence on acceleration for the slowest ramp (A). C,D) An expansion of Figure 3C,D between marks 2 and 7. Note that the slopes between marks 4 and 5 of these 2 curves are nearly identical.

Calculation of natural frequency and damping coefficient

The curve fitting of equation (1) was done for all ramp velocities. All velocities were presented twice with the exception of the fastest one which was presented once. These 11 different estimations of B and K values were paired and plotted against the 6 different velocities used (Figure 6. A,B). The elastic coefficient K varied from 0.25 to 0.32 Nm/deg linearly as a function of velocity (slope = 7.6×10^{-4} , i.e., the velocity dependent component of K is less than 20% at the peak test velocity of $100^\circ/\text{sec}$). The viscous coefficient B varied from 0.003 to 0.016 Nms/deg, but was nonlinearly related to velocity.

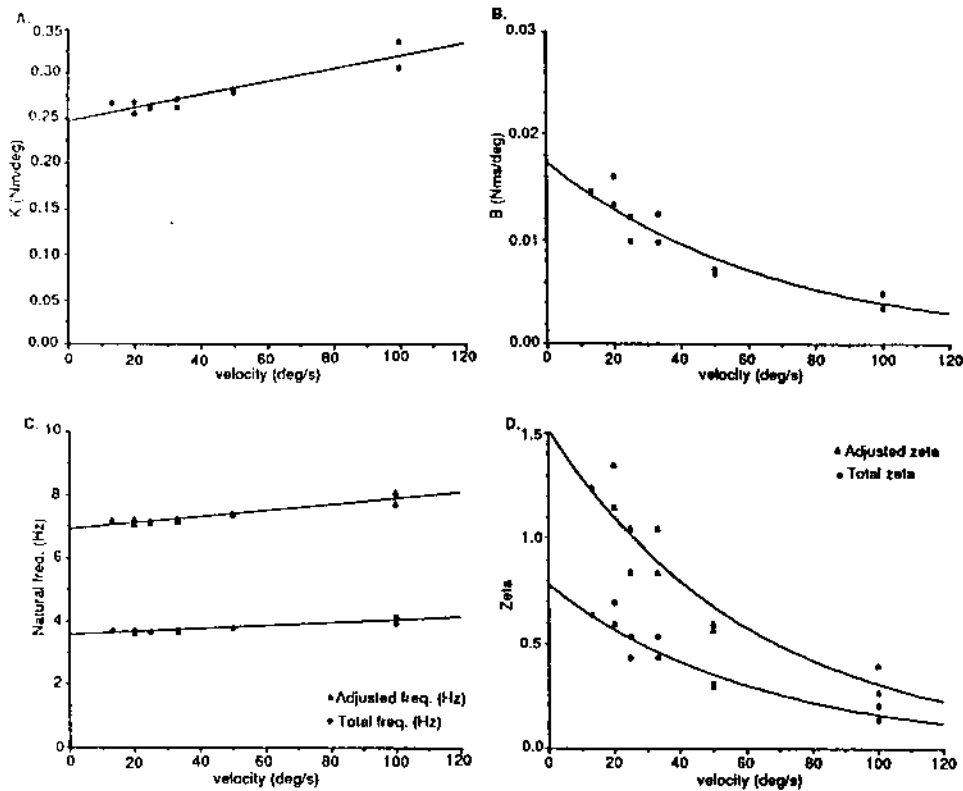


Figure 6. A,B) Calculated values for the stiffness coefficient, K , and the viscous damping coefficient, B , as functions of perturbation velocity. C) Plots of the natural frequency of the foot and testing device together, and of the foot alone (adjusted). D) Plots of the damping ratio, zeta, of the foot and testing device together, and of the foot alone (adjusted).

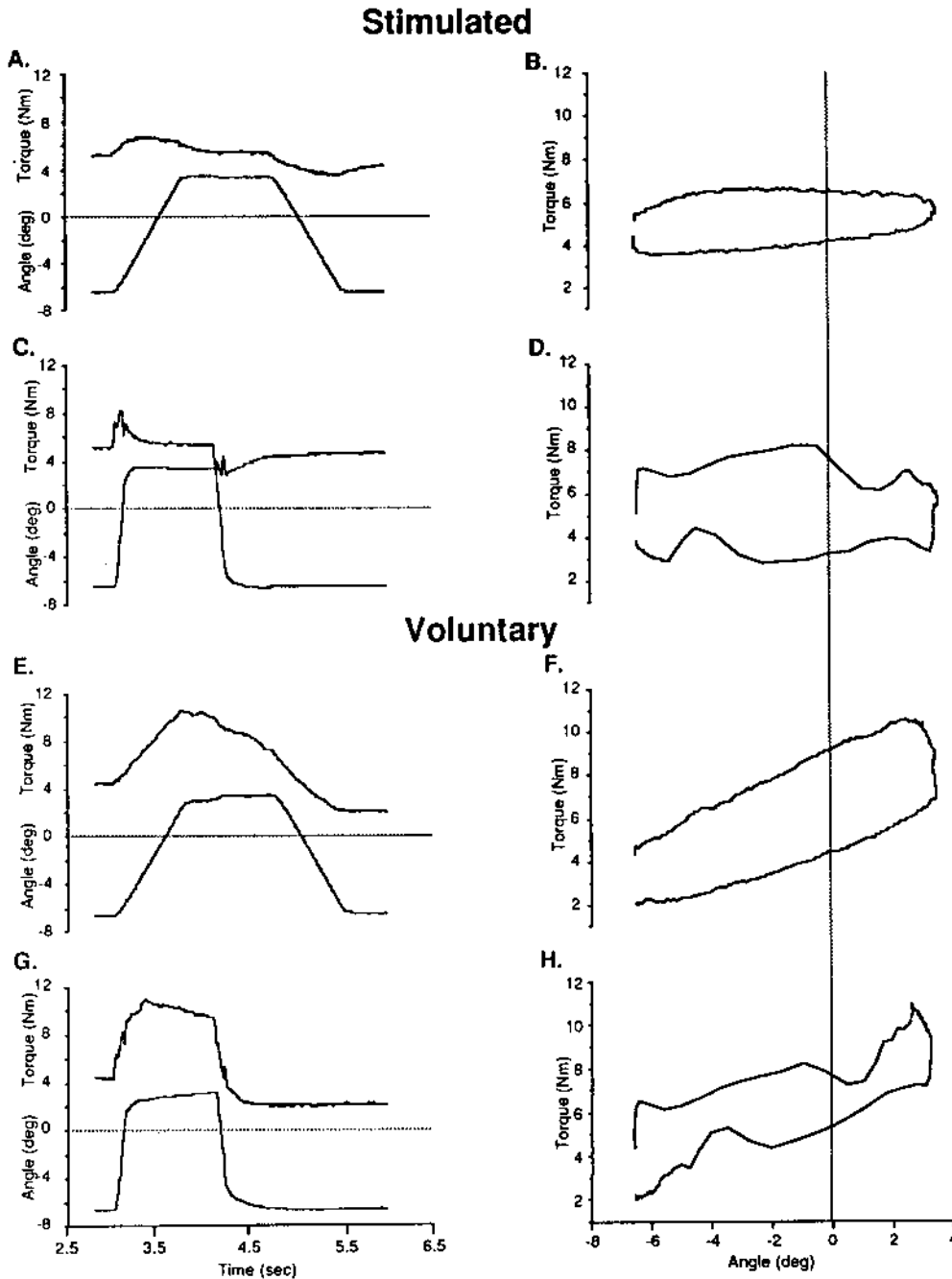


Figure 7. Torque and angular displacement profiles of a neurologically intact individual for slow (A,E) and fast (C,G) perturbations for bias torques achieved with electrical stimulation (A,C) or voluntarily (E,G). The corresponding plots of torque vs. angle are given in B,D,F and H.

From a knowledge of B and K , the change in natural frequency and damping coefficient as a function of velocity can be calculated from Equations (3) and (4). The lower curve in Figure 6C represents natural frequencies calculated from the combined inertia of the foot and the test device. From Equations (2) and (3), an adjusted natural frequency can be calculated for just the foot (upper curve in Figure 6C). Similarly, the damping coefficients can be plotted as a function of velocity. Again, the lower curve represents the influence of the combined inertia of the foot and test device. Since the test device has negligible B and K values, an adjusted damping coefficient can be calculated that arises only from the foot.

Comparison with results from a neurologically intact individual

Electrically Produced Bias Torque: The compliance characteristics of a neurologically intact subject during electrical stimulation were quite different from the complete paraplegic presented above. During the low velocity perturbation there was a nonlinear relationship between torque and angle (Figure 7B). The time series plot of this data (Figure 7A) shows that torque initially rises with displacement, but then decays back down to the pre-perturbation torque. Similar behavior is seen with the subsequent plantarflexion of the foot.

The high velocity perturbation shows a linear relationship between torque and angle (Figure 7D) for the first 100 msec, again, followed by a slow decay of torque back to the pre-perturbation level. The least squares estimation (8 points) of the stiffness coefficient (K) for the linear region of this curve is 0.337 ± 0.03 Nm/deg. The parameter values for the viscous coefficient are shown in Table 1.

	Stimulated, Paraplegic		Stimulated, Intact		Voluntary, Intact	
	slowest	fastest	slowest	fastest	slowest	fastest
B(Nms/deg)	0.0146	0.00347	0.0969*	0.0135	0.032	0.0181
K(Nm/deg)	0.265	0.337	0.0276*	0.307	0.476	0.387

Table 1. Estimated viscous damping and stiffness coefficient for Equation (1) for a complete paraplegic and a neurologically intact subject at highest and lowest perturbation velocities (* Estimation of this number is difficult due to nonlinear response of subject)

Voluntary Produced Bias Torque: A linear relationship between torque and angle was observed during the slowest perturbation during a voluntary torque bias (Figure 7F). The least squares estimation (92 data points) of the stiffness coefficient for this curve was estimated to be 0.674 ± 0.004 Nm/deg. During the hold portion of the perturbation the torque declined by about 4 Nm (Figure 7E). The resting torque, after the plantarflexion, portion of the perturbation, was about 2 Nm less than the pre-perturbation torque. This drop in torque and the torque drop during the hold portion of the perturbation are probably due to a voluntary correction made by the subject.

The high velocity perturbation during voluntary torque bias (Figure 7G,H) showed a linear relationship between torque and angle. The slope of this line was estimated to be 0.472 ± 0.025 Nm/deg (least squares estimation, 8 data points). Again, the torque declined (about 2 Nm) during the hold portion of the perturbation, and the final resting torque was less than the pre-perturbation torque, indicating a voluntary correction made by the subject. The parameter values for the viscous coefficient are shown in Table 1.

DISCUSSION

The parameter values for B and K for these three experiments are shown in Table 1. For comparison, the B and K values obtained by Agarwal and Gottlieb (5) for the ankle joint in normal human subjects using random perturbation inputs were: K ranged from 14.8 to 62.5 Nm/rad (ie. 0.258 to 1.09 Nm/deg) for different voluntary bias torques and B ranged from 0.234 to 0.631 Nm sec/rad (ie. 0.0041 to 0.011 Nm sec/deg). The numbers obtained from the current experiments are in agreement with those found previously by Agarwal and Gottlieb.

The constant velocity paradigm used in these experiments has several advantages over paradigms that control torque and let position vary. It minimizes the effects of the angle-dependent properties of the joint/muscle system since the displacement is always the same. Also, because the acceleration is near zero for a large portion of the perturbation, even for the highest velocities, we can directly observe the linearity of the system by plotting angle versus torque over the constant velocity region of the perturbation.

The compliance characteristics of the ankle of the paraplegic presented above are well described by Equation (1) for both the low and high velocity perturbations. The similarity of the stiffness coefficient (K) between the slowest and fastest perturbations (Table 1) indicates that the compliance characteristics of the joint during stimulation are primarily due to the passive properties of the joint. Thirteen years of disuse atrophy may be a significant contributing factor to this finding.

The change in the viscous damping (B) and stiffness (K) coefficients from the fastest to the slowest perturbation and the corresponding change in the natural frequency and damping coefficient (Figures 3C,D) could be due to either velocity dependent properties of the joint/muscle system or the contributions of spinal level reflexes during the slower perturbations. The high velocity perturbations are too brief for spinal level reflexes to have any effect on the measured viscous damping coefficient. However, as the velocity decreases, there is more time for the spinal level reflexes to have an effect. Further experiments are needed to separate the passive velocity dependent characteristics of the muscle/joint system from the reflex contributions.

The compliance characteristics of the neurologically intact subject presented here can not be adequately described by Equation (1) for the perturbations presented during stimulation. The torque versus angle plot (Figure 7B) can be separated into two regions. During the first 250 msec the torque is linearly related to the displacement. However, during the following 1.5 sec the torque decays back to the pre-perturbation levels. Similar decay is observed during the high velocity perturbations. This type of behavior requires a more complicated model than the one presented in Equation (1) and is a current area of research for the authors.

Acknowledgments: This research was funded by the U.S. Department of Veterans Affairs, Rehabilitation Research and Development Service, as Project B446-R. We thank Ron Cramer and Robert Kogel for their assistance on this project.

REFERENCES

1. Knafitz, M. and Merletti, R. "Suppression of Stimulation Artifacts from Myoelectric-Evoked Potential Recordings", *IEEE Transactions on Biomedical Engineering*: BME 35(9), 758-763, 1988.
2. Gottlieb, G. L. and Agarwal G. C. "Response to Sudden Torques About the Ankle in Man; Myotatic Reflex". *Journal of Neurophysiology*.Vol. 42 pp. 91-106, 1979.
3. Gottlieb, G. L. and Agarwal G. C. "Response to Sudden Torques About the Ankle in Man: II Postmyotatic Reaction." *Journal of Neurophysiology* Vol. 43 pp. 86-101, 1980.
4. Robinson, C. J., Flaherty, B., Agarwal, G. C., and Gottlieb, G. L., "Reflex Responses to Ankle Perturbations during Electrical Stimulation of Muscle: 1. Measurement Techniques and Preliminary Examples", *Annual Rocky Mountain Bioengineering Conference*, 1990.
5. Agarwal, G. C. and Gottlieb, G. L., "Compliance of the Human Ankle Joint" *ASME J. Biomechanics*, 99, 166-170, 1977.

Acknowledgments: This research was funded by the U.S. Department of Veterans Affairs, Rehabilitation Research and Development Service, as Project B446-R. We thank Ron Cramer and Robert Kogel for their assistance on this project.

REFERENCES

1. Knafitz, M. and Merletti, R. "Suppression of Stimulation Artifacts from Myoelectric-Evoked Potential Recordings", *IEEE Transactions on Biomedical Engineering*: BME 35(9), 758-763, 1988.
2. Gottlieb, G. L. and Agarwal G. C. "Response to Sudden Torques About the Ankle in Man; Myotatic Reflex". *Journal of Neurophysiology*.Vol. 42 pp. 91-106, 1979.
3. Gottlieb, G. L. and Agarwal G. C. "Response to Sudden Torques About the Ankle in Man: II Postmyotatic Reaction." *Journal of Neurophysiology* Vol. 43 pp. 86-101, 1980.
4. Robinson, C. J., Flaherty, B., Agarwal, G. C., and Gottlieb, G. L., "Reflex Responses to Ankle Perturbations during Electrical Stimulation of Muscle: 1. Measurement Techniques and Preliminary Examples", *Annual Rocky Mountain Bioengineering Conference*, 1990.
5. Agarwal, G. C. and Gottlieb, G. L., "Compliance of the Human Ankle Joint" *ASME J. Biomechanics*, 99, 166-170, 1977.